Molecular Cancer Therapeutics

JUN-Mediated Downregulation of EGFR Signaling Is Associated with Resistance to Gefitinib in EGFR-mutant NSCLC Cell Lines

Kian Kani[1,2], Carolina Garri[1], Katrin Tiemann[1], Paymaneh D. Malihi[1], Vasu Punj[3], Anthony L. Nguyen[1], Janet Lee[1], Lindsey D. Hughes[1], Ruth M. Alvarez[1], Damien M. Wood[1], Ah Young Joo[1], Jonathan E. Katz[1], David B. Agus[1,2], and Parag Mallick[1,4]

Abstract

Mutations or deletions in exons 18–21 in the *EGFR*) are present in approximately 15% of tumors in patients with non–small cell lung cancer (NSCLC). They lead to activation of the EGFR kinase domain and sensitivity to molecularly targeted therapeutics aimed at this domain (gefitinib or erlotinib). These drugs have demonstrated objective clinical response in many of these patients; however, invariably, all patients acquire resistance. To examine the molecular origins of resistance, we derived a set of gefitinib-resistant cells by exposing lung adenocarcinoma cell line, HCC827, with an activating mutation in the EGFR tyrosine kinase domain, to increasing gefitinib concentrations. Gefitinib-resistant cells acquired an increased expression and activation of JUN, a known oncogene involved in cancer progression. Ectopic overexpression of JUN in HCC827 cells increased gefitinib IC_{50} from 49 nmol/L to 8 μmol/L ($P < 0.001$). Downregulation of JUN expression through shRNA resensitized HCC827 cells to gefitinib (IC_{50} from 49 nmol/L to 2 nmol/L; $P < 0.01$). Inhibitors targeting JUN were 3-fold more effective in the gefitinib-resistant cells than in the parental cell line ($P < 0.01$). Analysis of gene expression in patient tumors with EGFR-activating mutations and poor response to erlotinib revealed a similar pattern as the top 260 differentially expressed genes in the gefitinib-resistant cells (Spearman correlation coefficient of 0.78, $P < 0.01$). These findings suggest that increased JUN expression and activity may contribute to gefitinib resistance in NSCLC and that JUN pathway therapeutics merit investigation as an alternate treatment strategy. *Mol Cancer Ther; 16(8); 1645–57. ©2017 AACR.*

Introduction

Lung cancer is a leading cause of cancer-related death worldwide (1). Patient outcomes are dependent on multiple factors, including the histologic subtype small-cell lung cancer (SCLC) versus non–small cell lung cancer (NSCLC), tumor stage, and the genomic signature of the tumor. These factors help to identify patients most likely to benefit from targeted therapeutics (2). For example, patients with EGFR-activating mutations have an increased likelihood of response to first-generation EGFR-targeted tyrosine kinase inhibitors (TKI) such as erlotinib and gefitinib (3, 4). Intrinsic or acquired resistance often limits the efficacy of targeted therapies (5, 6). Consequently, the median progression-free survival (PFS) time of patients treated with EGFR-targeted TKIs is 10–13 months (7).

Discerning a patient's EGFR mutation status and the mechanism of acquired resistance is critical for effective disease management. Resistance most often arises through secondary mutations in EGFR (T790M; ref. 8) or amplification of the *MET* oncogene (9), which account for 50% and 5% of the resistance mechanisms, respectively (10). A number of other mechanisms of acquired resistance have been identified in smaller percentages of patients (11). Approximately 30% of patients acquire resistance through mechanisms not yet elucidated (10).

In this study, we aimed to identify novel mechanisms of acquired resistance to gefitinib. We began our study with cell line models harboring EGFR-activating mutations or deletions. We created isogenic cell lines that were resistant to gefitinib. Next, we used multiple high-throughput screens to identify the mechanism of resistance to gefitinib. We found that upregulation of JUN was associated with the downregulation of the EGFR pathway because of coordinated changes in the stoichiometry and identity of the JUN interactome. The induction of JUN was independent of other AP1 transcription factors but required MAPK8 (JNK) activity to maintain the resistance phenotype. Unlike previously reported mechanisms of serine/threonine kinase activation of JUN (12), our resistant cells were sensitized to pharmacologic inhibition MAPK8, suggesting a MAPK8-mediated effect. Notably, a subset of NSCLC patients who did not have a sustained response to EGFR-targeted therapies exhibited the molecular phenotype associated with JUN upregulation.

[1]Lawrence J. Ellison Institute for Transformative Medicine, Keck School of Medicine, University of Southern California, Los Angeles, California. [2]Norris Comprehensive Cancer Center, Keck School of Medicine, University of Southern California Keck School of Medicine, Los Angeles, California. [3]Division of Hematology, Department of Medicine, University of Southern California, Los Angeles, California. [4]Department of Radiology, Stanford University, Stanford, California.

Note: Supplementary data for this article are available at Molecular Cancer Therapeutics Online (http://mct.aacrjournals.org/).

Corresponding Authors: Kian Kani, University of Southern California, 2250 Alcazar St., CSC140; CAMM, Los Angeles, CA 90033. Phone: 323-442-2539; Fax: 323-442-2539; E-mail: kani@usc.edu; and Parag Mallick, Stanford University, Stanford, CA 94305. E-mail: paragm@stanford.edu

doi: 10.1158/1535-7163.MCT-16-0564

Materials and Methods

Deposition of omics data

RNA-seq and ChIP-seq data has been submitted under GEO accession number GSE95592. Raw data files for the proteomics data have been deposited at (https://goo.gl/5zHj5b). Supplementary tables provide the complete searched data.

Reagents and cell lines

All chemicals were purchased from Sigma unless stated otherwise. Antibodies directed to EGFR, ERBB2, ERBB3, ERBB4, MET, MAPK8, p-EGFR (Y-1068), and scrambled shRNA and JUN shRNA were purchased from Santa Cruz Biotechnology. The antibodies to MAPK, pMAPK, AKT, pAKT, PTEN, YES, pYES, FOS, p-FOS, JUN-B, JUN-D, CREB, pCREB, CHK2, pCHK2, p38α, p-p38α, p-JUN, and SRC as well as EGF Receptor (D38B1) XP rabbit mAb (Sepharose Bead Conjugate) were obtained from Cell Signaling Technology. HCC827 (exon 19 del, E746-A750) and H3255 (exon 21 substitution, L858R), PC9 (exon 19 del), H4006 (exon 19 del), A431 (WT EGFR) cell lines were obtained from the ATCC and tested for mycoplasma (PCR) every 30 days. These cells were authenticated by ATCC utilizing short tandem repeat (STR) profiling and used within 6 months of purchase. Gefitinib, AS601245, JNK-IN-8, canertinib, and erlotinib were obtained from LC Labs. The CellTiter96 AQeous Non-Radioactive Cell Proliferation Assay (MTS) was purchased from Promega. The receptor and kinase array were obtained from R&D Systems and used according to the manufacturer's instructions.

Tissue culture experiments

HCC827 cells were cocultured in 10 nmol/L gefitinib for 1 month. The concentration of gefitinib was increased 3-fold every month. At 1 μmol/L gefitinib, the cells maintained growth with kinetics equal to that of the parental line. Three individual colonies from the HCC827 population were randomly selected and termed ZDR1-3. Sequencing was performed by Laragen Sequencing. Cell viability was assessed with the MTS assay. Briefly, cells were seeded at a density of 5,000 cells/well and treated with drug the next day. MTS reagent was added 24 to 48 hours later and analysis was performed as per the manufacturer's instructions. To assess drug response, cells were dosed with drug(s) for two hours and then incubated in 10 nmol/L *EGF* (Invitrogen) for 15 minutes prior to analysis.

The NSCLC cell lines HCC827 and H3255 were grown in DMEM (Invitrogen) containing 1% of dialyzed FBS (Invitrogen) and ^{13}C-lysine (100 mg/L) or ^{12}C -lysine (100 mg/L) for six passages according the standard SILAC protocol (13). Incorporation of ^{13}C-lysine exceeded 95% of the total protein lysine content. Total protein extracts were obtained by sonication of approximately 2×10^7 cells in 1 mL of PBS containing the detergent octyl-glucoside (1% w/v) and protease inhibitors (complete protease inhibitor cocktail, Roche Diagnostics) followed by centrifugation at 20,000 × *g*.

Verification

In vitro validation of proteomics data was accomplished by Western blot analysis. HCC827 parental cells and ZDR 1-3 were washed three times with PBS and lysed in RAF buffer with protease and phosphatase inhibitors supplemented with 1% SDS. Lysates were sonicated for 10 minutes, heated at 95°C for 10 minutes, and centrifuged for 15 minutes at 20,000 × *g*. The supernatant was cleared through a 0.22-μm filter and protein concentration was determined (BCA, Bio-Rad).

Chromatin immunoprecipitation

HCC827 cells were maintained on 15-cm plates until 80%–90% confluent. Cells were fixed using 1% formaldehyde for approximately 10 minutes at room temperature. Unreacted formaldehyde was quenched using 10× glycine solution provided with the EZ-Chip kit (Millipore, catalog no. 17-371). Cells were placed on ice and washed three times with 1× PBS solutions. Using a cell scraper, cells were collected and lysed using SDS lysis buffer and Protease Inhibitor Cocktail provided with the EZ-ChIP kit. Sonication conditions were optimized on a Covaris S2 sonicator to yield sheared crosslinked DNA between 200 and 1,000 base pairs in length. ChIP was performed using EZ-Chip protocol with the anti-JUN antibody from Santa Cruz Biotechnology (catalog no. SC-1694X). Normal mouse control IgG and anti-RNA polymerase II antibodies were provided with the kit (used as controls). PCR was performed with *GAPDH* primers to verify that ChIP controls.

RNA-seq and ChIP-seq

ChIP-seq was performed at the USC Epigenome Sequencing Core. Briefly, 200 ng of DNA was used to prepare ChIP and Input libraries. Libraries were generated using the Epicentre END-IT kit, the New England Biolabs A-tailing module, and Rapid Ligase from Enyzmatics following the manufacturer's protocols. Briefly, barcoded adapters were ligated and subjected to 10 to 14 rounds of PCR. Following PCR, reactions were cleaned using magnetic beads and resuspended in buffer. Libraries were quantified using the Kapa Biosystems Library Quantification Kit according to manufacturer's instructions. Libraries were applied to an Illumina flow cell and run on a HiSeq 2000. Image analysis and base-calling was carried out using RTA 1.13.48.0. Final file formatting, demultiplexing, and FASTQ generation was carried out using CASAVA v 1.8.2. For RNA-seq we used 50-bp single-end reads.

TCGA drug response expression and integration with HCC287-ZDR3 RNA-seq data

TCGA biospecimen and clinical information was obtained from https://tcga-data.nci.nih.gov/tcgafiles/ftp_auth/distro_ftpusers/anonymous/tumor/luad/bcr/biotab/clin/ or from OASIS (14). TCGA Illumina FASTQ sequencing data files were downloaded from the TCGA website (https://tcga -data.nci.nih.gov/tcga/tcgaDownload.jsp) and aligned using TopHat2 (15). The expression of each gene was measured as total RNA-seq reads uniquely mapped to the coding regions. Gene expression was then evaluated as described in the section "Bioinformatics analysis of RNA-seq data".

Gene set enrichment analysis

Gene set enrichment analysis (GSEA; ref. 16) was performed on a preranked list of differentially expressed genes as detailed previously (17). Gene sets tested for enrichment included all sets from the C2 collection of the GSEA Molecular Signatures Database v3.0.

A detailed description of DNA sequencing, cloning, and protein–protein interaction studies is provided in the Supplementary Methods and Materials section.

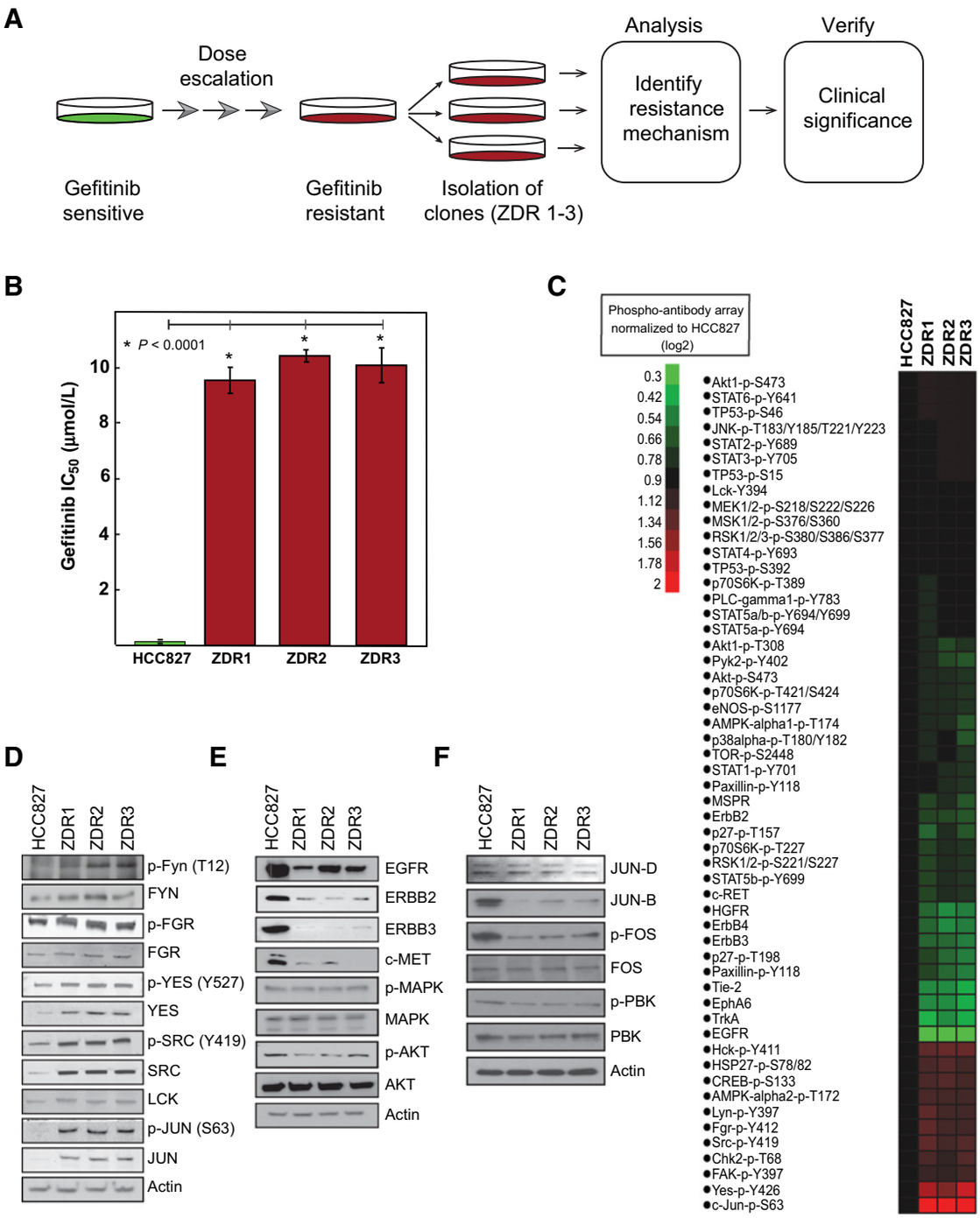

Figure 1.

Gefitinib-resistant phenotype is driven by SRC kinases or JUN. **A,** Schematic representation of experimental workflow. **B,** HCC827 parental and HCC827-ZDR clones were treated with gefitinib, and relative viability was assessed after 48 hours with MTS reagent. Plotted are means ± SDs of three biological replicates; asterisks indicate statistical significance ($P < 0.05$, Student t test). **C,** Heatmap of intensities of the signals from each phosphorylation site on phospho-antibody arrays (R&D Systems) normalized to signals in parental line. Phospho-antibody arrays were developed using secondary antibodies conjugated with a fluorescent reporter, and arrays were analyzed on the LI-COR imaging station. **D,** Representative immunoblots for the SRC kinases and JUN of whole-cell lysates of HCC827 cells and HCC827-ZDR clones. **E,** Representative immunoblots for total protein levels of indicated receptor tyrosine kinases and downstream signaling components from whole-cell lysates of HCC827 cells and HCC827-ZDR clones. One representative experiment of three is shown. **F,** Representative immunoblots for total protein levels of FOS, PBK, and JUNB/D from whole-cell lysates of HCC827 cells and HCC827-ZDR clones. One representative experiment of three is shown.

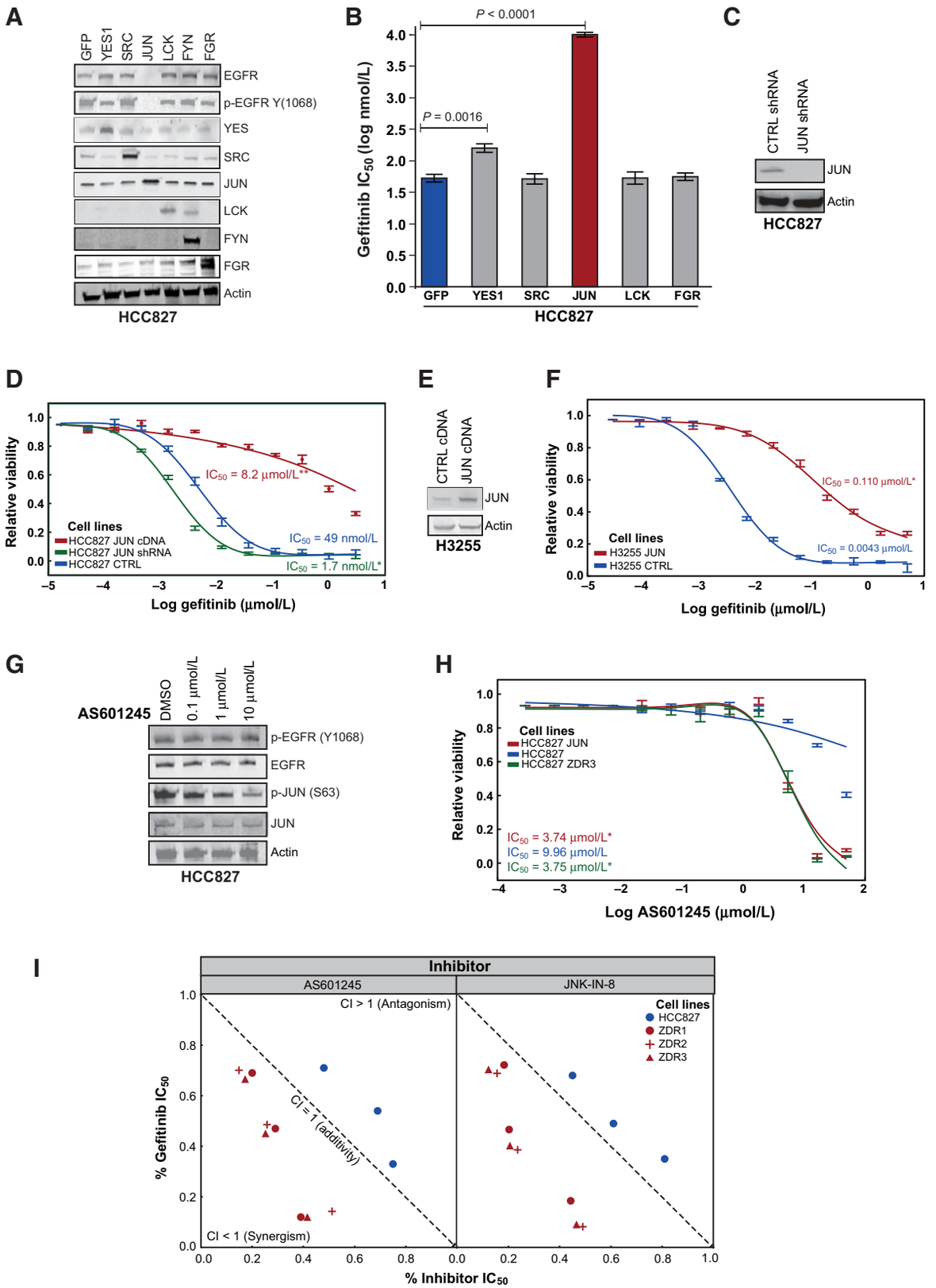

Results

Analysis of resistant NSCLC cell lines suggests a novel resistance mechanism

We derived a resistant pool of HCC827 (exon 19 del, E746-A750) cells by dose escalation of gefitinib to a final concentration of 1 μmol/L (Fig. 1A). Three individual clones were selected from the resistant pool and expanded separately when the population was able to survive a dose of 1 μmol/L gefitinib. Because ZD1839 was the original name for gefitinib, we named these resistant cell lines HCC827-ZDR. The HCC827-ZDR clones were significantly less sensitive to gefitinib than the parental line; the IC_{50} of gefitinib in the ZDR clones was approximately 9 μmol/L, whereas that in the parental cells was 49 nmol/L (Fig. 1B). To confirm that the shift in IC_{50} was not specific for gefitinib, we evaluated erlotinib and canertinib, two other TKIs that target EGFR (18). Erlotinib and canertinib inhibited growth of the parental line at nmol/L concentrations, whereas IC_{50}s when tested with the ZDR clones were greater than 10 μmol/L (Supplementary Fig. S1A).

To exclude previously documented mutations that could be the driving resistance mechanism in the HCC827-ZDR cells, we sequenced *EGFR*, *PI3CA*, and *BRAF*. We confirmed the EGFR-activating deletion (E746-A750) in the HCC827-ZDR cell lines, but we observed no additional EGFR mutations (Supplementary Fig. S1B and S1C). We also assessed EGFR phosphorylation as a function of gefitinib dosing by immunoblot. We observed a decrease in EGFR phosphorylation with gefitinib at concentrations that was comparable with that observed in the parental cell line (Supplementary Fig. S1D). This evidence suggests that secondary EGFR mutations are not driving resistance in the HCC827-ZDR cells.

We next used phospho-antibody arrays to identify differences in signal transduction pathways between the HCC827 and HCC827-ZDR cell lines. We used three phospho-antibody arrays, collectively enabling analysis of 114 phosphorylation sites in 92 proteins, including receptor tyrosine kinases ($n = 42$), MAPKs (24), and intracellular kinases ($n = 44$). We obtained quantifiable data on 48 unique phosphorylation sites (Fig. 1C). Relative to the parental line, we observed downregulation in approximately two-thirds of all phosphorylation sites in the HCC827-ZDR clones. We also detected downregulation in receptor tyrosine phosphorylation of EGFR, ERBB2, ERBB3, and MET in the gefitinib-resistant clones. However, we observed increased phosphorylation of the transcription factor JUN (4.1×) and the SRC family kinases [average fold change increase for SRC (2.6×), FGR (2.3×), LYN (0.7×), YES1 (3.1×), and LCK (1.4×)] in all three resistant clones relative to the parental cells. Interestingly, we did not observe differences in AKT or MAPK signaling.

We confirmed the results of the phospho-antibody array by performing immunoblots on cell lysates derived from the HCC827-ZDR cell lines (Fig. 1D). The immunoblots indicated a general upregulation in the phosphorylation and an increase in total protein for SRC kinases and JUN in the HCC827-ZDR cells relative to the HCC827 cells. Immunoblots also confirmed the downregulation of EGFR, ERBB2, ERBB3, and MET in the gefitinib-resistant cells (Fig. 1E).

The AP1 transcription unit is composed of JUN and FOS family members (19). Because of this, we interrogated the changes in JUN-B, JUN-D, and FOS in our resistant models. Western blot analysis demonstrated that the levels (JUN-B, JUN-D, FOS) and phosphorylation (p-FOS) are either unchanged or downregulated in the ZDR cell lines (Fig. 1F). To assess the impact of FOS overexpression on gefitinib resistance further, we created stable cell lines. We did not observe a change in gefitinib IC_{50} in these models (Supplementary Fig. S1F).

We also examined the level of the serine/threonine kinase [PBK (TOPK)] known to activate JUN in gefitinib resistance (12). Our data indicates that PBK and p-PBK are unperturbed in the ZDR models and are thus unlikely contributors to gefitinib resistance. Taken together, these findings indicate that the driving mechanism of resistance in the HCC827-ZDR lines was not any of the previously reported mechanisms (T790M in EGFR, MET, ERBB2, AXL, PI3CA, or BRAF). Furthermore, these results suggested that either SRC kinases or JUN facilitate gefitinib resistance.

JUN promotes resistance to gefitinib

SRC and JUN play crucial roles in signal transduction pathways and are involved in cell division, motility, adhesion, and survival in both normal and cancer cells (20, 21). Therefore, we wanted to determine whether the parental cell line would recapitulate the resistance phenotype by overexpression of SRC kinases or JUN. We created lentiviral constructs for expression of YES1, SRC, JUN, LCK, FYN, and FGR, and GFP (as a control) and transduced the parental HCC827 cell line with a multiplicity of infection (MOI = 5) to achieve physiologic levels of

Figure 2.

Expression of JUN is inversely correlated with sensitivity to gefitinib. **A,** HCC827 cells were transduced (MOI = 5) with viral particles carrying (GFP) or cDNA for expression of YES1, SRC, JUN, LCK, FYN, or FGR. The levels of each transgene and EGFR were assessed by immunoblot. One representative experiment of three is shown. **B,** Cell viability assays were used to determine the differential impact of overexpression of indicated genes on sensitivity to gefitinib. The IC_{50} values were calculated using a 4-parameter fit using that statistical package from JMP12 Pro. Each experiment was conducted at three separate time points with at least four technical replicates. Plotted are mean IC_{50} values ± 1 SD from three independent experiments. Probability associated with the Student *t* test is indicated when values are significant ($P < 0.05$). **C,** HCC827 cells were transduced with lentiviral particles for expression of control shRNA (targeting *GFP*) or shRNA targeting JUN. Levels of JUN were determined by immunoblot. **D,** The IC_{50} curve fit associated with the viability of HCC827 cells stably expressing GFP (blue), JUN (red), and JUN shRNA (green) as above. Statistical significance was assessed using the IC_{50} value from each replicate experiment. **E,** H3255 cells stably transfected for expression of control protein (GFP) or JUN were lysed and the degree of overexpression was determined by immunoblot. **F,** The IC_{50} curve fit associated with the viability of H3255 cells expressing GFP (blue) or JUN (red) as above. **G,** HCC827 cells were treated with AS601245 for 16 hours at the indicated concentrations. The cell lysate was analyzed by SDS-PAGE and immunoblot. **H,** The IC_{50} curve fit associated with the viability of HCC827-ZDR3 cells (green) and HCC827-ZDR3 cells that stably express GFP (blue) or JUN (red), treated with AS601245 for 48 hours. **I,** Inhibition of EGFR and MAPK8(JNK)/JUN pathway is synergistic only in the resistant cell lines. Cell viability assays were performed with both gefitinib and two JNK inhibitors (AS601245 and JNK-IN-08) to determine the synergistic, additive, or antagonistic effect of simultaneous dosing in the parental or ZDR cell lines. The resulting isobologram (48) was created by determining the IC_{20}, IC_{50}, IC_{80} of each drug alone and in combination. The mean (IC_{xx} values) of three experiments were calculated and an isobologram was drawn by JMP Pro12. The corresponding combination index (CI) values were calculated following the classic isobologram equation (48). Statistical significance was determined by using the Student t test ($P < 0.01$ for all of the points). As CI values of <1 express synergism, gefitinib+MAPK8 (JNK) inhibitors represents an example of a strongly synergistic combination in the resistant cell lines. The CI values for the parental cell line indicate a tendency toward antagonism (Student *t* test $P < 0.05$).

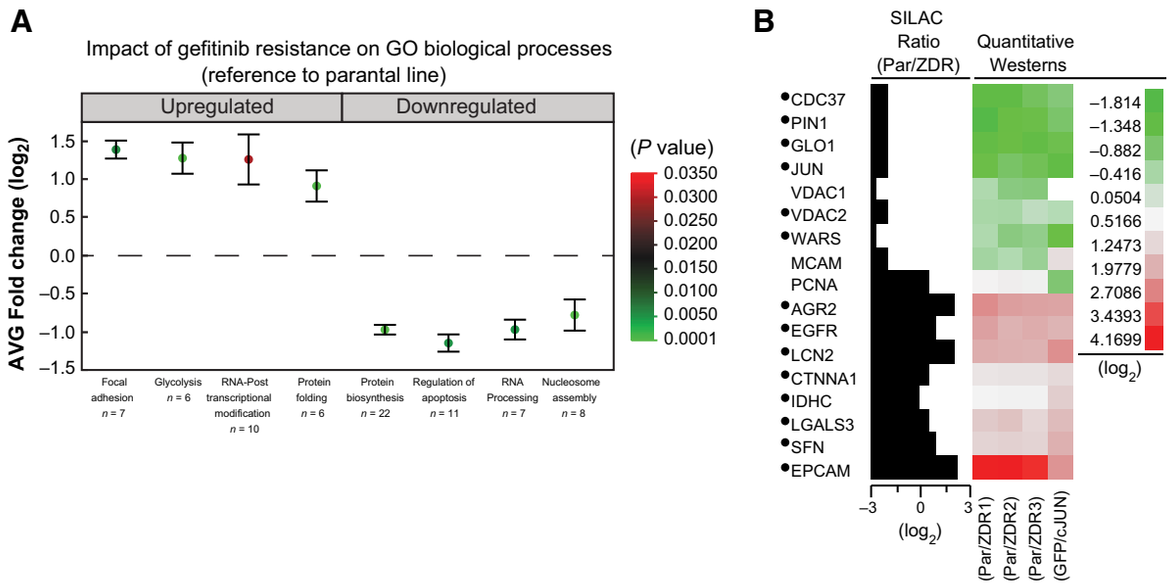

Figure 3.

HCC827-JUN–overexpressing cells share similar proteomic features to HCC827 gefitinib-resistant clones. **A,** Box plot of proteins that were up- or downregulated upon gefitinib resistance were subject to GO term enrichment analysis. The average fold change (log_2) and SD of the proteins belonging to an enriched GO biological process are included. The false discovery rate (*P* value) is represented by the color of each point. The number of proteins within each biological process, *n*, is listed next to each GO term. **B,** Cross-validation of quantitative proteomics data in HCC827 cells that stably overexpress JUN. Quantitative immunoblots that either confirmed the SILAC fold change of the proteins in the parental and ZDR cell lines or upon overexpression of JUN were used to generate a heatmap (raw data in Supplementary Fig. S3). The fold change for each protein is represented as the intensity of the immunoblot signal with respect to the parental cell line. The proteins identified with a bullet (•) show congruent fold change upon gefitinib resistance and JUN overexpression.

exogenous protein expression. Stable cell lines were created, and analysis of lysates by immunoblot indicated that we obtained moderate levels of each transgene (Fig. 2A). JUN overexpression led to decrease in the levels and phosphorylation of EGFR in HCC827 cells.

We performed cell viability experiments with each stable cell line to quantitatively evaluate gefitinib sensitivity as a function of SRC kinases and JUN overexpression (Fig. 2B). Our results indicated that overexpression of YES1 and JUN increase the gefitinib IC_{50}. The difference in IC_{50} between HCC827 cells that overexpress YES1 (148 nmol/L) and the parental cells (49 nmol/L) was not commensurate with the magnitude of the difference between the HCC827-ZDR clones (9 μmol/L) and the parental line. However, the difference between the parental line and the JUN-overexpressing HCC827 cells was of the same magnitude (from 49 nmol/L to 8.2 μmol/L) as the parental and the HCC827-ZDR cell lines (from 49 nmol/L to 9 μmol/L). We also examined the effects of inhibition of JUN expression on the sensitivity of the parental cell line to gefitinib. We utilized short hairpin RNA (shRNA) targeting JUN to reduce endogenous levels of the protein (Fig. 2C). The IC_{50} of the JUN shRNA cell line when treated with gefitinib was 1.7 nmol/L (Fig. 2D). These data indicated that levels of JUN inversely correlated with sensitivity to gefitinib in the HCC827 cell line.

To test the generality of our observation that JUN overexpression promotes resistance to gefitinib, we overexpressed JUN in the H3255 cell line. H3225 cells have an EGFR-L858R mutation, which is found in approximately 40% of NSCLC patients with EGFR-activating mutations (22). We observed that JUN overexpression (Fig. 2E) increased the gefitinib IC_{50} from 4 nmol/L to 110 nmol/L (Fig. 2F). In addition, we examined whether the phenotype of increased JUN expression led to downregulation of EGFR/p-EGFR by employing other models of gefitinib sensitivity. We overexpressed JUN in the PC9 (exon 19, del; E746–A750), H4006 (exon 19 del; L747 - E749, A750P), and A431 (WT EGFR) cell lines to assess its impact on EGFR. Both PC9 and H4006 cell lines demonstrated modest downregulation of EGFR/p-EGFR upon JUN overexpression (Supplementary Fig. S2A). We did not observe any changes in the EGFR in the A431 cell line.

MAPK8 inhibitors are useful tools for assessing the impact of JUN phosphorylation on cell growth (23). We first assessed the impact of a MAPK8 (JNK) inhibitor (AS601245) on the phosphorylation of EGFR and JUN (24). We treated HCC827, HCC827-ZDR3, and the HCC827-JUN cells with increasing concentrations of AS601245. We observed a dose-dependent downregulation of JUN phosphorylation without loss of EGFR phosphorylation in the parental cells (Fig. 2G). Moreover, inhibition of JUN phosphorylation did not affect growth of the parental cell line (Fig. 2H). AS601245 treatment, however, inhibited growth of the HCC827-ZDR3 and of the JUN-overexpressing HCC827 cell lines (Fig. 2H). We obtained similar results with an irreversible (JNK-IN-8) MAPK8 inhibitor (Supplementary Fig. S2B; ref. 25). We also investigated the impact of simultaneous dosing with gefitinib and MAPK8 inhibitors on the parental and gefitinib-resistant cell lines to assess the synergistic potential of these drugs. Pharmacologic inhibition of EGFR and MAPK8 (JNK) pathways was only synergistic in the HCC827-ZDR cell lines (Fig. 2I).

JUN overexpression recapitulates distinctive proteomic alterations present in ZDR cells

Our results suggest that upregulation of JUN can drive resistance to gefitinib. As JUN is a transcription factor, we hypothesized that the proteome of ZDR lines would be distinctly different from that of the parental cell line. To test this hypothesis, we first evaluated differences between the proteomes of the HCC827 cells and each of the three HCC827-ZDR clones by quantitative proteomics with stable isotope labeling with amino acids in culture (SILAC; ref. 13). In six separate runs, we identified 2,170 unique proteins (FDR < 1%; Supplementary Table S1), and we determined SILAC ratios (fold change $P < 0.05$) for 1,447 proteins. We analyzed the fold changes of fifteen proteins with SILAC ratios greater than $\pm$ 1.5 by immunoblot (Supplementary Fig. S3A) and the results confirmed the changes in the proteome of the resistant cell lines.

Gene ontology (GO) analysis (Fig. 3A) identified an upregulation of focal adhesion ($P = 0.006$), glycolysis ($P = 0.0002$), RNA posttranslational modification ($P = 0.03$), and protein folding ($P = 0.005$) in the gefitinib-resistant cell lines. Biological processes associated with protein biosynthesis ($P = 3 \times 10^{-12}$), regulation of apoptosis ($P = 0.005$), RNA processing ($P = 0.005$), and nucleosome assembly ($P = 7 \times 10^{-6}$) were downregulated in ZDR3 compared with parental cells. The IPA inference engine identified JUN as a key transcriptional regulator (Supplementary Figs. S4A).

As JUN expression appeared to be the major driver of the observed proteomics differences between our parental and HCC827-ZDR cell lines, we expected that JUN overexpression would generate a similar pattern of protein expression. The expression of the 14 validated proteins was compared in ZDR clones and the HCC827 cells that stably overexpress JUN by immunoblot. Twelve of these proteins showed similar fold changes relative to the corresponding parental cells (Fig. 3B; Supplementary Fig. S3B). In summary, overexpression of JUN was sufficient to exponentially increase gefitinib IC_{50}, lower EGFR levels and phosphorylation, and alter the proteome.

Reorganization of JUN-interacting partners modulates response to gefitinib

To both uncover potential upstream activators of JUN that may be complicit in resistance and better understand the connections between EGFR-MAPK8-JUN, we characterized the interacting partners for each protein in the HCC827 and HCC827-ZDR3 cell lines. We used affinity purification and subsequent identification of interacting proteins via mass spectrometry–based proteomic analysis (AP-MS). We utilized metabolic labeling and/or control (IgG) as reported previously (26) to minimize false identifications and to obtain quantitative information. We also utilized the CRAPome database to remove common contaminating proteins (27).

We started by comparing the impact of gefitinib and AS601245 dosing on the interaction between EGFR, MAPK8, and JUN. HCC827 and HCC827-ZDR3 cells dosed with either inhibitor demonstrated comparable downregulation of p-EGFR, p-MAPK8, and p-JUN (Fig. 4A). We conducted our co-immunoprecipitation (co-IP) while the cells were undosed to preserve native interacting partners for each protein (Supplementary Fig. S4D and S4E). The total number of interacting partners in the EGFR, MAPK8, JUN proteomes (Fig. 4B; Supplementary Table S2) qualitatively reflected their relative abundance in their respective cell lines (Fig. 1). Enrichment of GO terms derived from the EGFR and MAPK8 interactomes did not reveal any potential JUN activators (Supplementary Fig. S4B and S4C). Our AP-MS experiment identified 36 JUN-interacting proteins in the parental line and 97 in the resistant line (Supplementary Table S2, Supplementary Material and Methods). The number of quantified JUN peptides was 2-fold higher in the resistant line, qualitatively confirming the initial validation of the phospho-antibody arrays (Fig. 1C). To visualize the results of the AP-MS experiment, we separated proteins based on their membership in the parental (green), resistant (red), or both (blue) JUN interactome (Fig. 4C).

We separately analyzed the enrichment of GO terms associated with proteins unique to the parental and resistant cell lines. The proteins in the gefitinib-resistant JUN interactome were enriched for biological processes associated with protein folding, apoptosis, and glucose metabolism; we found a negative association for protein autophosphorylation ($P < 0.005$). Moreover, we observed a general increase in proteins associated with GTPase activity in the HCC827-ZDR3 cell line (Fig. 4E). This may indicate that the inhibition of kinase signaling causes a reorganization of the JUN interactome.

The AP-MS experiment also identified two JUN-interacting partners known to be negative regulators of EGFR activity, ERRFI1 and AGR2. ERRFI1 inhibits EGFR signaling by binding to the cytoplasmic tail of the receptor and interfering with its dimerization (28, 29). AGR2 prevents transport of EGFR to the cell surface and inhibits ligand-dependent activation (30, 31). Our analyses indicated an increase in the interaction between JUN and ERRFI1 and JUN and AGR2 in the resistant cell line compared with those in the HCC827 cells (Fig. 4D). The enrichment of JUN -interacting partners also highlighted proteins that modulate glucose metabolism (FOXA3), apoptosis (CREB), and the unfolded protein response (UPR) pathway (PDIA4 and CREB). A subsequent JUN coimmunoprecipitation experiment validated these findings (Fig. 4D). Taken together, our data indicate that a series of coordinated processes that rely on MAPK8 to activate JUN may drive gefitinib resistance. During this process, we observed a redistribution of interacting partners known to mediate downregulation of EGFR activity.

Acquired resistance to gefitinib is accompanied by distinct JUN chromatin occupancy

We hypothesized that the reorganization of the JUN interactome should be accompanied by increased transcriptional activity and promoter occupancy of JUN-regulated genes in the resistant line. We chose the HCC827-ZDR3 clone at random to serve as the surrogate model for our resistance mechanism. We were confident of this choice because all three HCC827-ZDR cell lines had similar phospho-array signatures, proteomic profiles, and responses to gefitinib. We utilized the Illumina Hi-Seq 2000 platform with 50XPE reads to study the gene expression of the HCC827 parental and HCC827-ZDR3 cell lines. Supplementary Table S3 tabulates the top 260 differentially expressed gene (Fig. 5A). We validated the fold changes of several of these genes by RT-PCR (Supplementary Fig. S5A).

Gene set enrichment analysis (GSEA) revealed a correlation of this gene set with genes previously reported to be involved in gefitinib resistance (32), cancer metastasis (33), cell migration (34), and CDH1 targets (ref. 35; Fig. 5B). IPA revealed enrichment in pathways associated with cell movement, regulation of proliferation, cell death, and metabolism (Supplementary Fig. S5B). We also noted that 23 of the 260 genes were linked previously to EGFR signaling (Supplementary Table S4). On average, the absolute fold change based on normalized reads per kilobase per million mapped reads (RPKM) levels of these 23 genes were decreased in

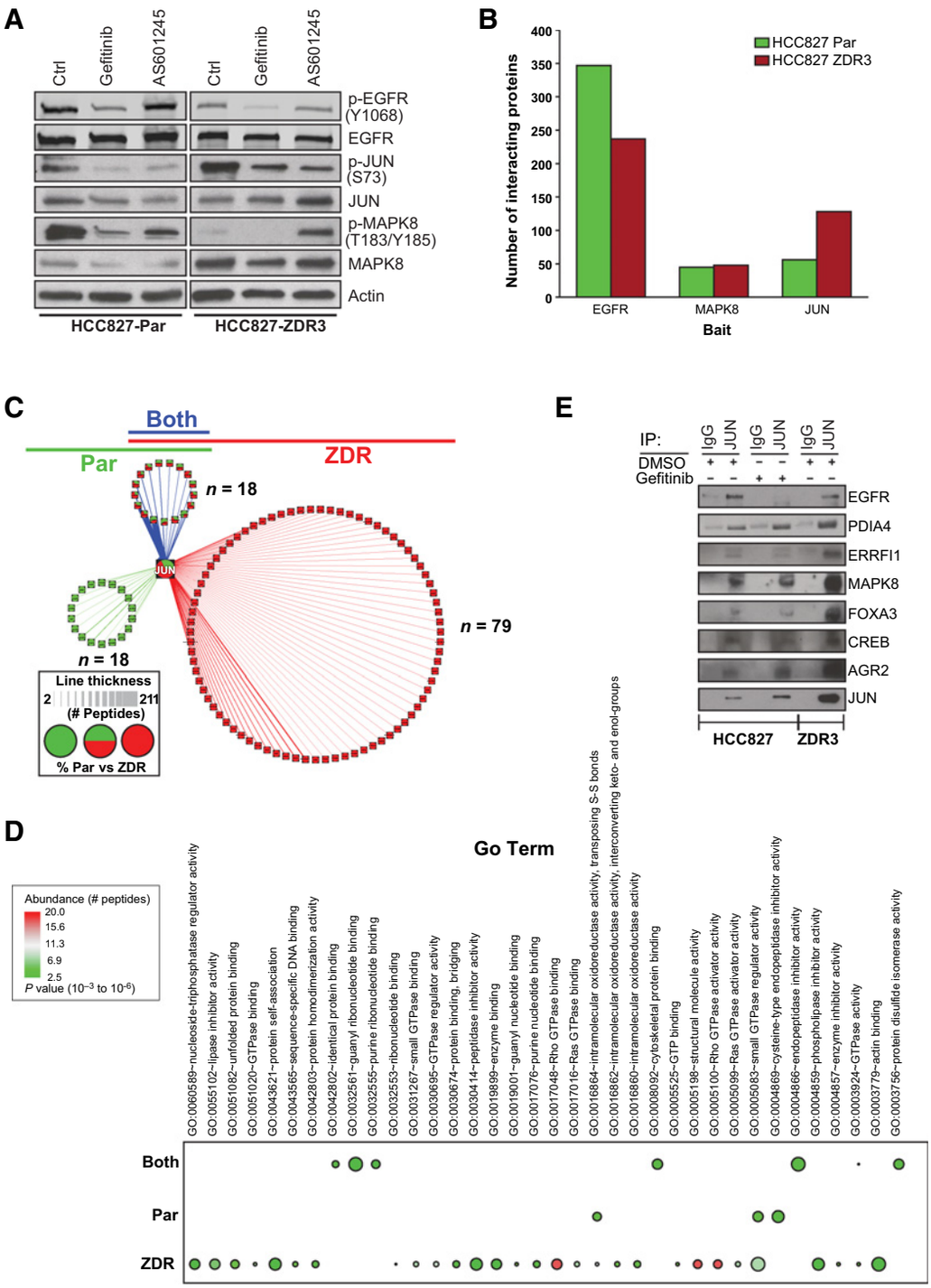

Figure 4.

JUN interactomes differ in parental and HCC827-ZDR cells. **A,** Response to treatment with gefitinib and MAPK8 (JNK) inhibitor (AS601245) in HCC827 and HCC827-ZDR3 cell lines. **B,** Co-IP was used to identify JUN, EGFR, and MAPK8-interacting proteins in parental (green) and resistant (red) cell lines. **C,** AP-MS was used to identify JUN proteins in parental (green) and resistant (red) cell lines. Proteins that were identified in both cell lines are colored blue. The thickness of the line represents the number of peptides detected. Pie charts indicate proportions of peptides that were identified in each interactome for proteins identified in both cell lines. **D,** Co-IP of JUN in HCC827 and HCC827-ZDR3 cells treated with gefitinib (1 μmol/L) or vehicle control (DMSO) for 16 hours. **E,** GO enrichment of JUN-interacting proteins identified in both the parental and ZDR3 cell lines. The proteins that were identified in the JUN co-IP experiments were separated into three groups based on the following membership (identified only in parental, ZDR, or both cell lines). GO enrichment was used to identify biological process that were either unique or shared among each group. The abundance of each protein within each group was derived from the number of times each protein was identified (FDR < 0.01) and is depicted on the basis of the color of each bullet. The Benjamini-adjusted FDR is indicated by the size of each bullet.

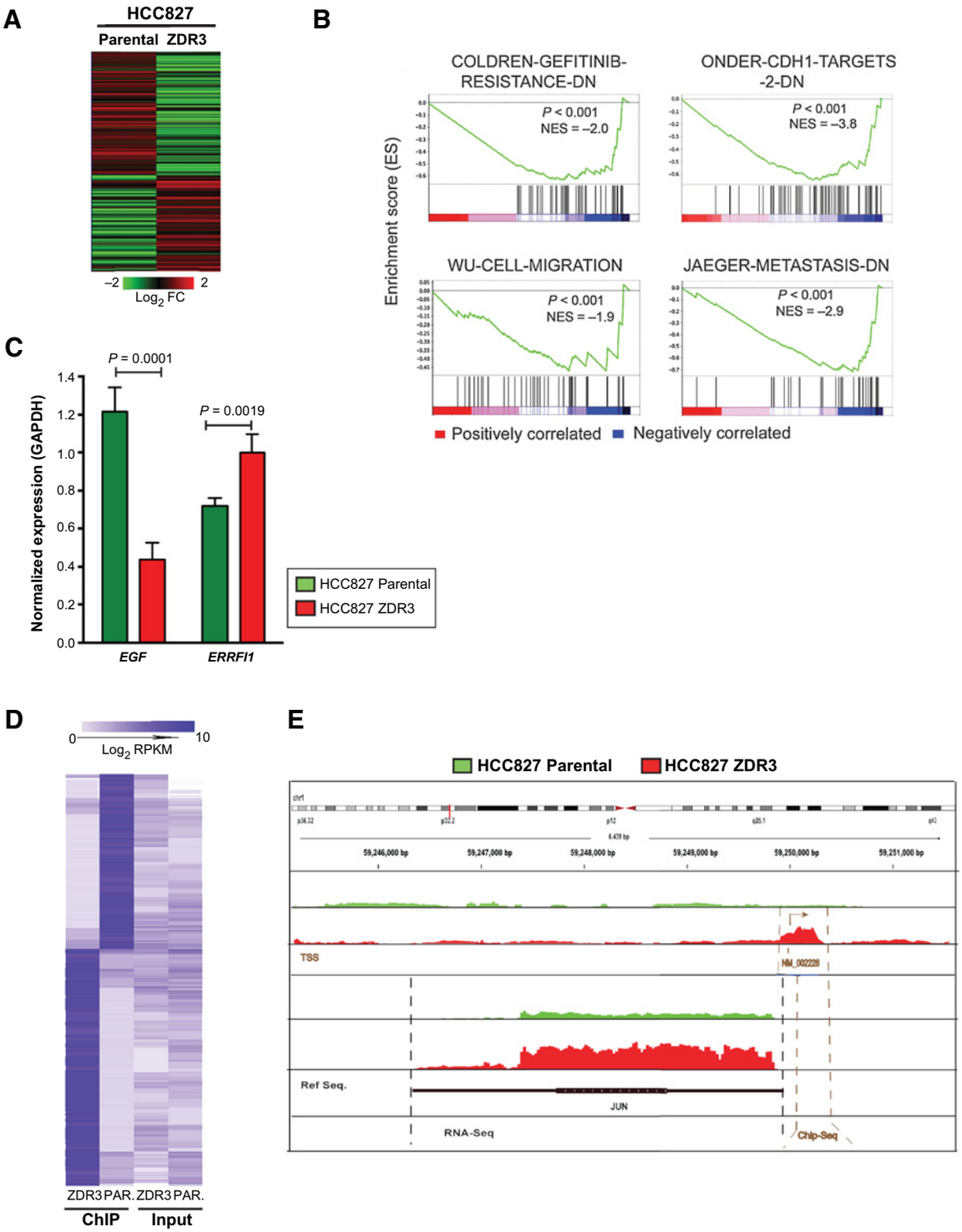

Figure 5.

JUN expression promotes downregulation of EGFR activity via altered chromatin occupancy. **A,** Heatmap of differential expression of genes in HCC827 parental and ZDR3 resistant cells (260 genes with $\log_2$ fold change in expression of $\pm$ 2.0; $P < 0.05$). **B,** Gene set enrichment analysis of 260 genes across various clinical datasets were ranked by a signal-to-noise metric representing their differential expression. The color of the gradient represents either positive (red) or negative (blue) correlation with the listed gene sets. **C,** RT-qPCR analysis of *EGF* and *ERBBFI1* expression in HCC827 and HCC827-ZDR cells normalized on the basis of the expression of *GAPDH*. Significance was set at a $P < 0.05$. **D,** The 1,488 genes identified as differentially enriched in a JUN ChIP-seq experiment were subject to hierarchical clustering based on Euclidean distance and average linkage. **E,** Genomic map of JUN chromosomal occupancy. Red indicates enrichment in the ZDR3 line; green indicates enrichment in the parental line.

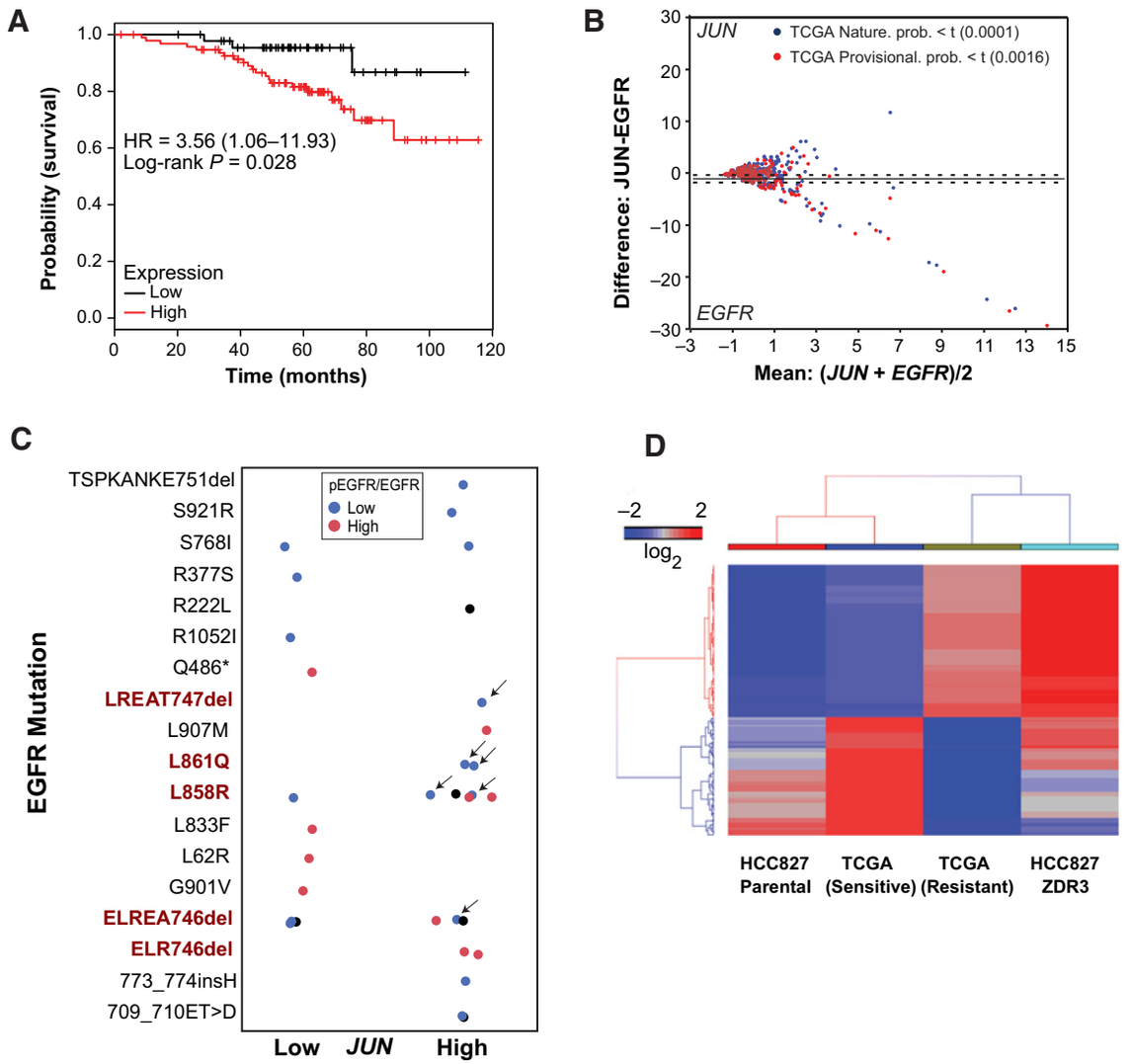

Figure 6.

JUN overexpression has clinical relevance. **A,** Kaplan–Meier analysis of the probability of survival as a function of relative expression of JUN in a cohort of 147 lung adenocarcinoma tumors derived from patients without a smoking history. The 201464_x_at probe set was used for the analysis on KMPLOT (49). **B,** Correlations of *JUN* and *EGFR* expression in independent cohorts of patients with NSCLC (BioPortal, Provisional NSCLC, 2014; ref. 50). Statistical significance was assessed by ANOVA. **C,** Patients in these two clinical cohorts with mutations in EGFR were selected. Known EGFR-activating mutations are in red text. Normalized *JUN* RNA-seq read counts and p-EGFR/EGFR values from antibody arrays are plotted as a function of *JUN* expression. Patients with EGFR-activating mutations, high *JUN* expression, and low phosphorylation are indicated by arrows. **D,** Clinical response and gene expression in patients who were responsive or resistant to EGFR-targeted therapy (erlotinib or gefitinib). The genes were subject to hierarchical clustering with the Euclidean distance and average linkage was used for clustering (Spearman rank correlation coefficient of 0.78, $P < 0.01$). Expression values were calculated as $\log_2$ from RNA-seq read counts.

the ZDR3 cells relative to the parental cells (average fold change of -0.92). We validated the downregulation of *EGF* and upregulation of *ERRFI1* by quantitative RT-PCR in the ZDR3 cell line compared with the parental cells (Fig. 5C). Thus, the EGFR pathway is systematically downregulated because of JUN upregulation in the gefitinib-resistant cell lines.

Genome-wide ChIP-seq performed with an anti-JUN antibody indicated a distinct enrichment in ChIP-seq tag density in ZDR3 cells relative to parental cells in the 4-kilobases on either side of transcription start sites of known JUN-regulated genes (Supplementary Fig. S5C). A total of 494 genes with a $\log_2$ fold change of $\pm$ 2 were identified when the HCC827 cell profile was compared with the HCC827-ZDR profile (Supplementary Table S5; Fig. 5D). We confirmed the results of the ChIP-seq experiment by performing RT-qPCR on the input and antibody enriched (IgG and JUN) fractions. The data confirmed the distinct chromatin binding pattern between the parental and ZDR cell line (Supplementary Fig. S5D). As our data indicated an upregulation in levels of JUN protein (Fig. 1D) and RNA (Supplementary Table S3), we specifically examined the occupancy of JUN at its own promoter. Higher levels of occupancy of JUN at the JUN transcription start site as shown by ChIP-seq and a concomitant higher level of JUN

Table 1. Correlation between JUN expression and ratio of phosphorylated versus total EGFR

		NSCLC (Provisional)		NSCLC (Nature)	
p-EGFR/EGFR	Count (*n*)	Mean difference	Mean Mean	Mean difference	Mean Mean
Low	91	−0.077	−0.062	−1.641	1.0678
High	90	−2.472	1.2484	−0.058	0.2248
F Ratio		16.562	19.981	7.9296	8.923
P > F		0.0001	0.0001	0.0054	0.0032

NOTE: MANOVA (JUN expression in patients with high or low p-EGFR/EGFR ratio). The NSCLS (Provisional) was obtained from refs. 36 and 37 (Nature).

mRNA expression as shown by RNA-seq were observed in the ZDR cells compared with HCC827 cells (Fig. 5E). This suggests that a positive feedback loop maintains a high basal level of JUN in the gefitinib-resistant cell line. We also discovered that JUN occupies a region upstream of the *ERRFI1* promoter in both the parental and resistant cells with 2-fold higher levels of chromatin occupancy in the resistant line (Supplementary Table S5).

Upregulation of JUN is associated with decreased EGFR activity and resistance to EGFR TKIs in patients with NSCLC

We next investigated the correlation between patient prognosis and JUN expression. NSCLC patients without prior history of smoking had poorer outcomes with elevated expression of JUN (Fig. 6A). Because our data indicated a potential inverse relationship between JUN expression and EGFR expression, we also interrogated two independent clinical datasets from the Cancer Genome Atlas (TCGA) database with genomic and phosphoproteomic readouts (36, 37). In both datasets, we observed an inverse correlation between EGFR and JUN expression (Fig. 6B). We also utilized the normalized RNA-seq read counts and p-EGFR/EGFR values from antibody arrays from the above two datasets to discriminate the difference between mean values in patients with high or low p-EGFR/EGFR. In these two independent datasets, we also observed a statistically significant association between EGFR activity (as inferred based on phosphorylation) and JUN levels (Table 1). As we derived our cell-based data from NSCLC cell lines with activating EGFR mutations, we specifically analyzed EGFR phosphorylation (Y1068) status and JUN levels in patients with EGFR-activating mutations. We selected patients with mutations in EGFR from these two clinical cohorts. We identified patients with EGFR-activating mutations, high JUN expression, and low levels of phosphorylation of EGFR (Fig. 6C).

We also used TCGA datasets of lung adenocarcinoma from OASIS (Pfizer Oncology group) to examine the correlation between EGFR activating mutations and JUN (14). Of the 520 lung tumors, 80 samples had mutations in the EGFR gene with corresponding JUN expression either by RNA-seq or gene array. Of these 80 EGFR-mutant samples, 56% showed overexpression of JUN over the median TPM (transcript per million) JUN expression. On the contrary, in case of wild-type EGFR, 62% of samples showed downregulation of JUN expression. We subsequently investigated individual patients in TCGA with activating EGFR mutations who received either gefitinib or erlotinib (38). We excluded patients with the EGFR T790M and with *MET* amplifications and evaluated the remaining patients for expression of the 260 genes differentially expressed in the HCC827-ZDR cells compared with the parental cells. Our investigation revealed that the gene expression pattern of our parental cell line closely resembles that of a responsive patient, whereas the gene expression profile of our gefitinib-resistant cells matches the expression profile of a patient who is refractory to treatment (Fig. 6D).

Discussion

Characterization of HCC827-ZDR gefitinib-resistant cell lines showed that a possible mechanism underlying resistance was upregulation of the JUN oncogene. We confirmed that upregulation of JUN drove resistance to gefitinib by utilizing a combination of genomic, pharmacologic, and proteomic tools. Genomic manipulation of JUN levels in the HCC827 and H3255 NSCLC cell lines revealed an inverse correlation between sensitivity to gefitinib and JUN activity. Our data also revealed that downregulation of EGFR levels and activity was concomitant with upregulation of JUN activity in the PC9 and H4006 cell line and in patient lung cancer samples. This is clinically relevant because our data indicates that lung cancer patients with this mode of resistance may not benefit from second- or third-generation EGFR-targeted TKIs. Instead, a combination of EGFR-targeted and MAPK8/JUN-targeted therapies might provide improved clinical outcome for these patients (Fig. 2I). Activation of MAPK8 has been previously reported as a potential bypass mechanism in lung cancer cell lines that are addicted to EGFR (39). Inhibitors of the MAPK8/JUN pathway are in development clinically for the treatment of inflammation, neurologic disorders, and cancer (40). The combination of MAPK8/JUN and EGFR pathway inhibitors merits clinical investigation in this lung cancer patient population.

The inverse correlation between sensitivity to EGFR TKIs and JUN levels likely results from reorganization of the JUN interactome, increased JUN binding at distinct transcription start sites, and differential gene and protein expression. Our co-IP data indicated that JUN forms protein complexes with EGFR and MAPK8 when EGFR is phosphorylated (Supplementary Fig. S4D); thus, the MAPK8/JUN pathway is downstream of EGFR signaling in the HCC827 cells. This confirms the findings of previous studies that have linked the activation of receptor tyrosine kinases to JUN transcriptional activity (41). Other groups have also reported a receptor tyrosine kinase independent mode of JUN activation (42). The capacity to reformulate signaling pathways in response to chronic drug treatment seems to be a hallmark of therapeutic resistance.

The exact mechanism that triggers increased MAPK8 (JNK) activity in the TKI-resistant cells is unknown. The levels of other AP1 components (JUN-B, JUN-D, and FOS) are either unchanged or downregulated in our resistance model. As our mode of resistance is also independent of PBK, we separately enumerated the interactome of EGFR, MAPK8, FOS (Supplementary Fig. S1G and S1H), and JUN in the parental and resistant cell lines to identify candidate proteins that may be complicit in resistance. A systematic evaluation of these proteins may provide greater insight into the molecular mechanism governing JUN activity. JUN may be "activated" by at least two distinct mechanisms in the HCC827-ZDR cell lines. The first involves phosphorylation in its N-terminal region by

MAPK8. As MAPK8 is a substrate of MAPKs, a number of different pathways may govern its activity. The results of our AP-MS experiments indicated that the common feature between the JUN interactomes in the parental and resistant cell lines were proteins that are involved in GTPase regulation. This suggests that certain GTPases may regulate the activity of MAPK8 in the gefitinib-resistant cells. Induction of transcription through intrinsic or extrinsic stimuli may also activate JUN (43). Our ChIP-seq data demonstrated significantly increased binding of JUN at its own promoter and we observed higher levels of JUN mRNA and JUN protein in the HCC827-ZDR cells compared with the parental cells. Thus, both transcriptional and posttranscriptional regulation modulates JUN-mediated resistance to gefitinib. A recent report by Fallahi-Sichani and colleagues noted that upregulation of JUN is sufficient to promote resistance to BRAF inhibitors, hinting at a shared escape pathway (44).

Although targeted therapy has resulted in improved prognosis in several tumor types, including lung cancers with therapeutics that target molecular pathways such as EGFR and ALK, tumor cells invariably develop resistance. A number of studies are investigating combination therapy, differential dosing, and the use of second- and third-generation drugs to overcome resistance (45–47). Our identification of JUN-mediated acquired resistance will motivate improved patient theranostics and may ultimately lead to new treatment options.

Disclosure of Potential Conflicts of Interest

No potential conflicts of interest were disclosed.

Authors' Contributions

Conception and design: K. Kani, A.L. Nguyen, D.B. Agus, P. Mallick
Development of methodology: K. Kani, A.L. Nguyen, D.B. Agus, P. Mallick
Acquisition of data (provided animals, acquired and managed patients, provided facilities, etc.): K. Kani, C. Garri, P.D. Malihi, A.L. Nguyen, J. Lee, L.D. Hughes, R.M. Alvarez, D.M. Wood, A.Y. Joo, J.E. Katz
Analysis and interpretation of data (e.g., statistical analysis, biostatistics, computational analysis): K. Kani, C. Garri, K. Tiemann, V. Punj, A.L. Nguyen, J.E. Katz, D.B. Agus
Writing, review, and/or revision of the manuscript: K. Kani, C. Garri, K. Tiemann, A.L. Nguyen, D.B. Agus, P. Mallick
Administrative, technical, or material support (i.e., reporting or organizing data, constructing databases): K. Kani, P. Mallick
Study supervision: D.B. Agus, P. Mallick

Acknowledgments

We are grateful for the generous financial support of the Wunderkinder Foundation, Redstone Family Foundation, and Lawrence J. Ellison. We appreciate the support of Autumn Beemer and Lisa Flashner leading to the generation and publication of this manuscript. We thank Laura Ng for administrative support.

Grant Support

This work was supported by the NIH/NCI grants CCNE-T U54 U54CA151459 (to D.B. Agus) and CCNE-TR U54 CA119367 (to D.B. Agus).

The costs of publication of this article were defrayed in part by the payment of page charges. This article must therefore be hereby marked *advertisement* in accordance with 18 U.S.C. Section 1734 solely to indicate this fact.

Received August 25, 2016; revised March 8, 2017; accepted May 8, 2017; published OnlineFirst May 31, 2017.

References

1. Ferlay J, Soerjomataram I, Dikshit R, Eser S, Mathers C, Rebelo M, et al. Cancer incidence and mortality worldwide: sources, methods and major patterns in GLOBOCAN 2012. Int J Cancer 2015;136:E359–86.
2. Pao W, Miller V, Zakowski M, Doherty J, Politi K, Sarkaria I, et al. EGF receptor gene mutations are common in lung cancers from "never smokers" and are associated with sensitivity of tumors to gefitinib and erlotinib. Proc Natl Acad Sci U S A 2004;101:13306–11.
3. Shiau CJ, Babwah JP, da Cunha Santos G, Sykes JR, Boerner SL, Geddie WR, et al. Sample features associated with success rates in population-based EGFR mutation testing. J Thorac Oncol 2014;9:947–56.
4. Dungo RT, Keating GM. Afatinib: first global approval. Drugs 2013;73:1503–15.
5. Paez JG, Janne PA, Lee JC, Tracy S, Greulich H, Gabriel S, et al. EGFR mutations in lung cancer: correlation with clinical response to gefitinib therapy. Science 2004;304:1497–500.
6. Kobayashi S, Boggon TJ, Dayaram T, Janne PA, Kocher O, Meyerson M, et al. EGFR mutation and resistance of non-small-cell lung cancer to gefitinib. N Engl J Med 2005;352:786–92.
7. Mok TS, Wu YL, Thongprasert S, Yang CH, Chu DT, Saijo N, et al. Gefitinib or carboplatin-paclitaxel in pulmonary adenocarcinoma. N Engl J Med 2009;361:947–57.
8. Pao W, Miller VA, Politi KA, Riely GJ, Somwar R, Zakowski MF, et al. Acquired resistance of lung adenocarcinomas to gefitinib or erlotinib is associated with a second mutation in the EGFR kinase domain. PLoS Med 2005;2:e73.
9. Engelman JA, Zejnullahu K, Mitsudomi T, Song Y, Hyland C, Park JO, et al. MET amplification leads to gefitinib resistance in lung cancer by activating ERBB3 signaling. Science 2007;316:1039–43.
10. Sequist LV, Waltman BA, Dias-Santagata D, Digumarthy S, Turke AB, Fidias P, et al. Genotypic and histological evolution of lung cancers acquiring resistance to EGFR inhibitors. Sci Transl Med 2011;3:75ra26.
11. Stewart EL, Tan SZ, Liu G, Tsao MS. Known and putative mechanisms of resistance to EGFR targeted therapies in NSCLC patients with EGFR mutations-a review. Transl Lung Cancer Res 2015;4:67–81.
12. Li Y, Yang Z, Li W, Xu S, Wang T, Niu M, et al. TOPK promotes lung cancer resistance to EGFR tyrosine kinase inhibitors by phosphorylating and activating c-Jun. Oncotarget 2016;7:6748–64.
13. Ong SE, Blagoev B, Kratchmarova I, Kristensen DB, Steen H, Pandey A, et al. Stable isotope labeling by amino acids in cell culture, SILAC, as a simple and accurate approach to expression proteomics. Mol Cell Proteomics 2002;1:376–86.
14. Fernandez-Banet J, Esposito A, Coffin S, Horvath IB, Estrella H, Schefzick S, et al. OASIS: web-based platform for exploring cancer multi-omics data. Nat Methods 2016;13:9–10.
15. Kim D, Pertea G, Trapnell C, Pimentel H, Kelley R, Salzberg SL. TopHat2: accurate alignment of transcriptomes in the presence of insertions, deletions and gene fusions. Genome Biol 2013;14:R36.
16. Mootha VK, Lindgren CM, Eriksson KF, Subramanian A, Sihag S, Lehar J, et al. PGC-1alpha-responsive genes involved in oxidative phosphorylation are coordinately downregulated in human diabetes. Nat Genet 2003;34:267–73.
17. Punj V, Matta H, Chaudhary PM. A computational profiling of changes in gene expression and transcription factors induced by vFLIP K13 in primary effusion lymphoma. PLoS One 2012;7:e37498.
18. Avizienyte E, Ward RA, Garner AP. Comparison of the EGFR resistance mutation profiles generated by EGFR-targeted tyrosine kinase inhibitors and the impact of drug combinations. Biochem J 2008;415:197–206.
19. Ryseck RP, Bravo R. c-JUN, JUN B, and JUN D differ in their binding affinities to AP-1 and CRE consensus sequences: effect of FOS proteins. Oncogene 1991;6:533–42.
20. Parsons SJ, Parsons JT. Src family kinases, key regulators of signal transduction. Oncogene 2004;23:7906–9.
21. Leppa S, Bohmann D. Diverse functions of JNK signaling and c-Jun in stress response and apoptosis. Oncogene 1999;18:6158–62.
22. Pao W, Wang TY, Riely GJ, Miller VA, Pan Q, Ladanyi M, et al. KRAS mutations and primary resistance of lung adenocarcinomas to gefitinib or erlotinib. PLoS Med 2005;2:e17.

23. Bogoyevitch MA.Therapeutic promise of JNK ATP-noncompetitive inhibitors. Trends Mol Med 2005;11:232–9.
24. Carboni S, Hiver A, Szyndralewiez C, Gaillard P, Gotteland JP, Vitte PA. AS601245 (1,3-benzothiazol-2-yl (2-[[2-(3-pyridinyl) ethyl] amino]-4 pyrimidinyl) acetonitrile): a c-Jun NH2-terminal protein kinase inhibitor with neuroprotective properties. J Pharmacol Exp Ther 2004;310:25–32.
25. Zhang T, Inesta-Vaquera F, Niepel M, Zhang J, Ficarro SB, Machleidt T, et al. Discovery of potent and selective covalent inhibitors of JNK. Chem Biol 2012;19:140–54.
26. Tackett AJ, DeGrasse JA, Sekedat MD, Oeffinger M, Rout MP, Chait BT. I-DIRT, a general method for distinguishing between specific and nonspecific protein interactions. J Proteome Res 2005;4:1752–6.
27. Mellacheruvu D, Wright Z, Couzens AL, Lambert JP, St-Denis NA, Li T, et al. The CRAPome: a contaminant repository for affinity purification-mass spectrometry data. Nat Methods 2013;10:730–6.
28. Ferby I, Reschke M, Kudlacek O, Knyazev P, Pante G, Amann K, et al. Mig6 is a negative regulator of EGF receptor-mediated skin morphogenesis and tumor formation. Nat Med 2006;12:568–73.
29. Zhang X, Pickin KA, Bose R, Jura N, Cole PA, Kuriyan J. Inhibition of the EGF receptor by binding of MIG6 to an activating kinase domain interface. Nature 2007;450:741–4.
30. Dong A, Gupta A, Pai RK, Tun M, Lowe AW. The human adenocarcinoma-associated gene, AGR2, induces expression of amphiregulin through Hippo pathway co-activator YAP1 activation. J Biol Chem 2011;286:18301–10.
31. Dong A, Wodziak D, Lowe AW. Epidermal growth factor receptor (EGFR) signaling requires a specific endoplasmic reticulum thioredoxin for the post-translational control of receptor presentation to the cell surface. J Biol Chem 2015;290:8016–27.
32. Coldren CD, Helfrich BA, Witta SE, Sugita M, Lapadat R, Zeng C, et al. Baseline gene expression predicts sensitivity to gefitinib in non-small cell lung cancer cell lines. Mol Cancer Res 2006;4:521–8.
33. Wu Y, Siadaty MS, Berens ME, Hampton GM, Theodorescu D. Overlapping gene expression profiles of cell migration and tumor invasion in human bladder cancer identify metallothionein 1E and nicotinamide N-methyltransferase as novel regulators of cell migration. Oncogene 2008;27:6679–89.
34. Jaeger J, Koczan D, Thiesen HJ, Ibrahim SM, Gross G, Spang R, et al. Gene expression signatures for tumor progression, tumor subtype, and tumor thickness in laser-microdissected melanoma tissues. Clin Cancer Res 2007;13:806–15.
35. Onder TT, Gupta PB, Mani SA, Yang J, Lander ES, Weinberg RA. Loss of E-cadherin promotes metastasis via multiple downstream transcriptional pathways. Cancer Res 2008;68:3645–54.
36. Cerami E, Gao J, Dogrusoz U, Gross BE, Sumer SO, Aksoy BA, et al. The cBio cancer genomics portal: an open platform for exploring multidimensional cancer genomics data. Cancer Discov 2012;2:401–4.
37. Gao J, Aksoy BA, Dogrusoz U, Dresdner G, Gross B, Sumer SO, et al. Integrative analysis of complex cancer genomics and clinical profiles using the cBioPortal. Sci Signal 2013;6:pl1.
38. Lee HJ, Zhuang G, Cao Y, Du P, Kim HJ, Settleman J. Drug resistance via feedback activation of Stat3 in oncogene-addicted cancer cells. Cancer Cell 2014;26:207–21.
39. Manole S, Richards EJ, Meyer AS. JNK Pathway Activation Modulates Acquired Resistance to EGFR/HER2-Targeted Therapies. Cancer Res 2016;76:5219–28.
40. Clarke N, Arenzana N, Hai T, Minden A, Prywes R. Epidermal growth factor induction of the c-jun promoter by a Rac pathway. Mol Cell Biol 1998;18:1065–73.
41. Barr RK, Bogoyevitch MA. The c-Jun N-terminal protein kinase family of mitogen-activated protein kinases (JNK MAPKs). Int J Biochem Cell Biol 2001;33:1047–63.
42. Xia Z, Dickens M, Raingeaud J, Davis RJ, Greenberg ME. Opposing effects of ERK and JNK-p38 MAP kinases on apoptosis. Science 1995; 270:1326–31.
43. Lamph WW, Wamsley P, Sassone-Corsi P, Verma IM. Induction of proto-oncogene JUN/AP-1 by serum and TPA. Nature 1988;334:629–31.
44. Fallahi-Sichani M, Moerke NJ, Niepel M, Zhang T, Gray NS, Sorger PK. Systematic analysis of BRAFV600E melanomas reveals a role for JNK/c-Jun pathway in adaptive resistance to drug-induced apoptosis. Mol Syst Biol 2015;11:797.
45. Cross DA, Ashton SE, Ghiorghiu S, Eberlein C, Nebhan CA, Spitzler PJ, et al. AZD9291, an irreversible EGFR TKI, overcomes T790M-mediated resistance to EGFR inhibitors in lung cancer. Cancer Discov 2014;4: 1046–61.
46. Planchard D, Loriot Y, Andre F, Gobert A, Auger N, Lacroix L, et al. EGFR-independent mechanisms of acquired resistance to AZD9291 in EGFR T790M-positive NSCLC patients. Ann Oncol 2015;26:2073–8.
47. Walter AO, Sjin RT, Haringsma HJ, Ohashi K, Sun J, Lee K, et al. Discovery of a mutant-selective covalent inhibitor of EGFR that overcomes T790M-mediated resistance in NSCLC. Cancer Discov 2013;3:1404–15.
48. Tallarida RJ. Drug synergism: its detection and applications. J Pharmacol Exp Ther 2001;298:865–72.
49. Gyorffy B, Surowiak P, Budczies J, Lanczky A. Online survival analysis software to assess the prognostic value of biomarkers using transcriptomic data in non-small-cell lung cancer. PLoS One 2013;8:e82241.
50. Comprehensive molecular profiling of lung adenocarcinoma. Nature 2014;511:543–50.